Temporal and spatial distributions of precipitation on the Huang-Huai-Hai Plain during 1960–2019, China

Minhua Ling, Hongbao Han, Xingling Wei and Cuimei Lv

ABSTRACT

The Huang-Huai-Hai Plain is an important commercial grain production base in China. Understanding the temporal and spatial variations in precipitation can help prevent drought and flood disasters and ensure food security. Based on the precipitation data for the Huang-Huai-Hai Plain from 1960 to 2019, this study analysed the spatiotemporal distribution of total precipitation at different time scales using the Mann–Kendall test, the wavelet analysis, the empirical orthogonal function (EOF), and the centre-of-gravity model. The results were as follows: (1) The winter precipitation showed a significant upward trend on the Huang-Huai-Hai Plain, while other seasonal trends were not significant. (2) The precipitation on the Huang-Huai-Hai Plain shows a zonal decreasing distribution from southeast to northwest. (3) The application of the EOF method revealed the temporal and spatial distribution characteristics of the precipitation field. The cumulative variance contribution rate of the first two eigenvectors reached 51.5%, revealing two typical distribution fields, namely a 'global pattern' and a 'north-south pattern'. The 'global pattern' is the decisive mode, indicating that precipitation on the Huang-Huai-Hai Plain is affected by large-scale weather systems. (4) The annual precipitation barycentres on the Huang-Huai-Hai Plain were located in Jining city and Taian city, Shandong Province, and the spatial distribution pattern was north-south. The annual precipitation barycentres tended to move southwest, but the trend was not obvious. The annual precipitation barycentre is expected to continue to shift to the north in 2020.

Key words | EOF, Huang-Huai-Hai Plain, Mann–Kendall test, precipitation barycentre, wavelet analysis

Minhua Ling
Hongbao Han
Xingling Wei
Cuimei Lv (corresponding author)
School of Water Conservancy Engineering,
Zhengzhou University,
Zhengzhou 450001,
China
E-mail: *lvcuimei305@163.com*

Minhua Ling
Yellow River Institute for Ecological Protection & Regional Coordinated Development,
Zhengzhou University,
Zhengzhou 450001,
China
and
Zhengzhou Key Laboratory of Water Resource and Environment,
Zhengzhou 450001,
China

HIGHLIGHTS

- Temporal and spatial variation characteristics of total precipitation on the Huang-Huai-Hai Plain.
- Two typical distribution fields on the Huang-Huai-Hai Plain.
- The shifts of precipitation barycentres on the Huang-Huai-Hai Plain.

doi: 10.2166/wcc.2021.313

GRAPHICAL ABSTRACT

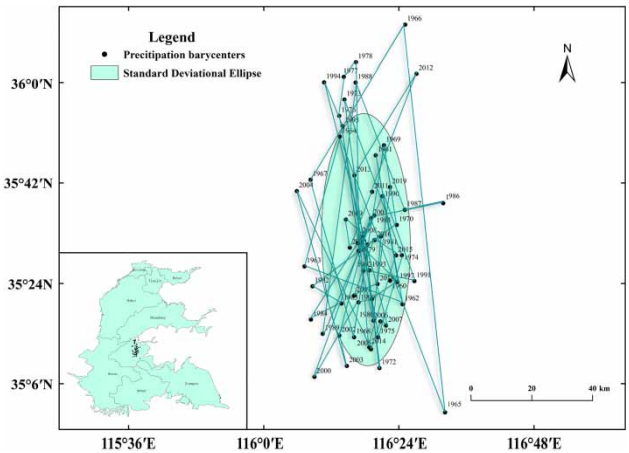

INTRODUCTION

In recent years, the global climate has been abnormal, and the surface temperature has continued to increase. Droughts, heavy rains, and floods have occurred frequently and have been widely distributed and severe (Costa & Soares 2009). Precipitation is an important indicator to describe the climate characteristics of a specific area. The temporal and spatial distributions of precipitation directly affect the regional hydrological situation and the temporal and spatial distributions of water resources (Aziz & Burn 2005). In the research on the impact of climate change on China's water cycle and water resources, many studies have been carried out in the past 20 years and some new insights have been obtained. For example, the study found that the national average annual precipitation in the past half-century has exhibited obvious decadal and multi-decadal fluctuations (Liu *et al.* 2005a, 2005b; Ren *et al.* 2005). Although the overall trend of precipitation in China is not obvious, the spatial difference is significant. Precipitation decreases in the central and southern parts of Northeast China, North China, Central China, and Southwest China, while precipitation increases in the southeast coast, the lower reaches of the Yangtze River, the Tibetan Plateau, and Northwest China (You *et al.* 2011; Li *et al.* 2012). The reasons for precipitation fluctuations from decade to multi-decade are generally believed to be mainly related to the variation of the ocean–atmosphere coupling mode and the variation of the East Asian monsoon system (Qian *et al.* 2007). As to the reasons for the long-term trend of precipitation in some regions, some studies believe that it may be related to global warming (Li & Luo 2011). The Huang-Huai-Hai Plain is located in eastern China. The plain has a warm temperate monsoon climate with co-occurring rain and heat, and it is a vital commodity grain base in China. Affected by climate change, precipitation on the Huang-Huai-Hai Plain showed a decreasing trend and the degree of temporal and spatial variability increased. This has further aggravated the tight water shortage situation (Rong & Luo 2009), seriously threatening the area's agricultural production and the safety of residents' domestic water (Zhang *et al.* 2015). Therefore, understanding the characteristics of the temporal and spatial changes in precipitation is of great significance to the assessment and management of water resources, flood control and drought relief, and agricultural arrangements on the Huang-Huai-Hai Plain (Worku *et al.* 2019).

Drought poses a serious threat to food production. Many scholars have conducted research on the drought, dry, and wet conditions on the Huang-Huai-Hai Plain. Based on the monthly standardized precipitation index (SPI) on a long-term scale (12 and 36 months), Wu *et al.* (2011) analysed the

temporal and spatial differentiation of the dry and wet conditions on the Huang-Huai-Hai Plain. Li *et al.* (2017) analysed the spatial and temporal distributions of drought characteristics on the Huang-Huai-Hai Plain based on the standardized precipitation evapotranspiration index (SPEI). They found that the past 50 years have experienced reduced drought of shorter duration, and of weaker severity and intensity. Research on total precipitation and extreme precipitation are very important in hydrology, especially from the perspective of agriculture, such as early warning of agricultural droughts and floods, allocation of irrigation water, and ensuring food production (Li *et al.* 2018). At present, the research on the temporal and spatial variation characteristics of precipitation on the Huang-Huai-Hai Plain mainly focuses on extreme precipitation. Zhang *et al.* (2008) analysed the temporal and spatial characteristics of the frequency of extreme precipitation events in the North China Plain in the past 45 years. An *et al.* (2013) calculated the precipitation, frequency, and intensity of extreme precipitation events and found that extreme precipitation events on the Huang-Huai-Hai Plain showed an overall downward trend in the past 50 years. Based on four extreme precipitation indexes, Fang *et al.* (2018) analysed the temporal and spatial characteristics of extreme precipitation on the Huang-Huai-Hai Plain. However, there are few studies on the temporal and spatial variation characteristics of total precipitation on the Huang-Huai-Hai Plain. The precipitation barycentre can reveal the overall distribution characteristics of regional precipitation. Its dynamic trajectory reflects the dispersion, transfer, and dominant distribution of precipitation, which is helpful when analysing the differences in and balance of regional precipitation (Luo *et al.* 2015). However, current research on the distribution and shifts in precipitation barycentres on the Huang-Huai-Hai Plain is relatively lacking.

Based on monthly precipitation data on the Huang-Huai-Hai Plain over the past 60 years, this paper analysed the temporal and spatial characteristics of total precipitation in the study area and revealed the migration of the precipitation barycentre in the past 60 years using the M-K test, wavelet analysis, the empirical orthogonal function (EOF), and the centre-of-gravity model. This study is expected to provide references for the sustainable use of water resources, agricultural production, and disaster prevention on the Huang-Huai-Hai Plain.

DATA AND METHODS

Study region

The Huang-Huai-Hai Plain is located between 32–40°N and 112–121°E, with a plain area of 3.1×10^5 km^2 (27% of the total plain area in China), and it includes most or part of five provinces (Hebei, Henan, Shandong, Anhui, and Jiangsu) and two cities (Beijing and Tianjin). The Huang-Huai-Hai Plain has been the political, economic, and cultural centre of China since ancient times and has a current population of 339 million, accounting for 24.2% of China's total population, and both the area of arable land and the gross domestic product (GDP) account for approximately one-quarter of the overall values in China. The Huang-Huai-Hai Plain is bounded by the T'ai-hang Mountains and Funiu Mountain in the west, the Bohai Sea and Yellow River in the east, the Yanshan Mountains in the north, and the Ta-pieh Mountains in the south. The Huang-Huai-Hai Plain is the second largest plain in China and is a typical alluvial plain. It has a vast area and low terrain, most of which is below 50 m above sea level. The eastern coastal plain is below 10 m above sea level. The Huang-Huai-Hai Plain is an area of China that is sensitive and vulnerable to climate change. It has a warm temperate monsoon climate, with obvious changes in the four seasons, the co-occurrence of rain and heat, and frequent droughts and floods. The annual precipitation is 545.6–1,007.6 mm, with more than 70% falling in summer and autumn (Zhang *et al.* 2011). The heat on the Huang-Huai-Hai Plain is suitable for two crops a year. The primary planting method is a winter wheat–summer maize rotation. The planting areas of wheat and corn account for 61 and 31%, respectively, of the country's total (Yang *et al.* 2015), making it an important commercial grain production base in China (Yuan *et al.* 2019). The locations of the Huang-Huai-Hai Plain and the meteorological stations used in this study are shown in Figure 1.

Data sources

This study selects monthly precipitation data from 215 meteorological stations on the Huang-Huai-Hai Plain from

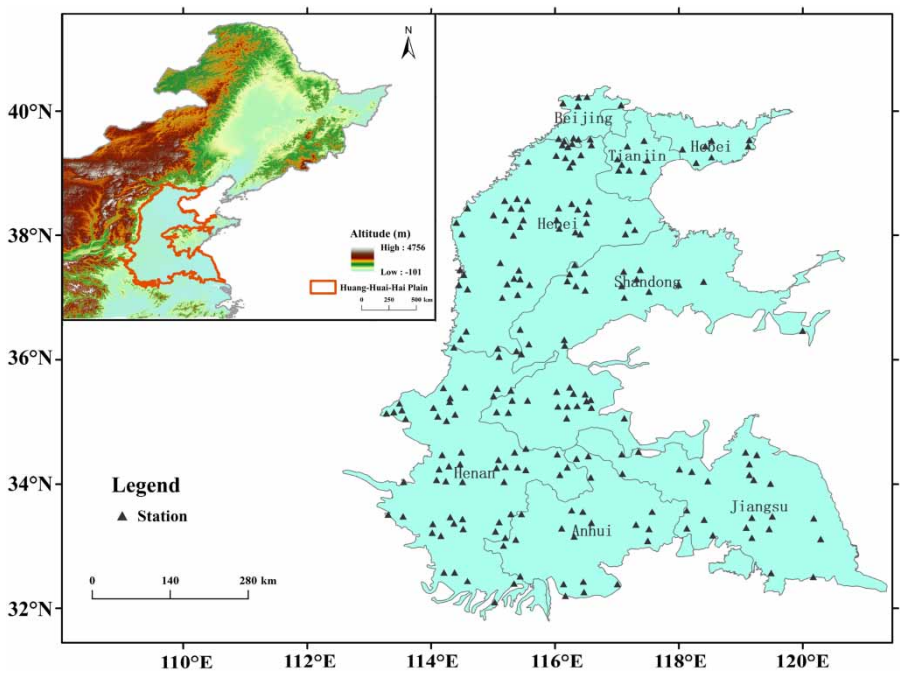

Figure 1 | Location of the Huang-Huai-Hai Plain and the meteorological stations used in this study.

1960 to 2019. Monthly precipitation data are sourced from the digitized data of the 'Monthly Statement of Ground Meteorological Records' (http://data.cma.cn/). The data have undergone the quality control of the National Meteorological Administration. The data used have no missing values and are of good quality. According to the climatic characteristics of the Huang-Huai-Hai Plain, spring is specified as the period from March to May, summer is the period from June to August, autumn is the period from September to November, and winter is the period from December to February of the following year. The annual and four-season precipitation on the Huang-Huai-Hai Plain is the areal rainfall calculated by weighting the precipitation at 215 stations according to the Tyson polygon method.

Methods

Mann–Kendall test

The Mann–Kendall (M-K) test is a nonparametric statistical test method. This method does not need to consider the sample distribution law or whether there are abnormal values, and it is suitable for testing hydrological and meteorological data (Yu *et al.* 2002; Pirnia *et al.* 2019). The specific calculation formulas are as follows:

$$s = \sum_{i=1}^{n} \sum_{j=1}^{i-1} \mathrm{sign}(x_i - x_j) \tag{1}$$

$$\mathrm{sign}(x_i - x_j) = \begin{cases} -1 & (x_i - x_j) < 0 \\ 0 & (x_i - x_j) = 0 \\ 1 & (x_i - x_j) > 0 \end{cases} \tag{2}$$

$$Z = \begin{cases} (s-1)/\sqrt{(n(n-1)(2n+5))/18}, & S > 0 \\ 0, & S = 0 \\ (s+1)/\sqrt{(n(n-1)(2n+5))/18}, & S < 0 \end{cases} \tag{3}$$

where if Z is greater than 0, the sample data shows an increasing trend, and if Z is less than 0, the sample data shows a decreasing trend. At $|Z|$ values greater than or equal to 1.28, 1.64, and 2.32, the sample data has passed the significance test with a reliability of 90, 95, and 99%, respectively.

Wavelet analysis

Wavelet analysis is a method of local time-frequency analysis proposed by the geologist Morlet in the 1980s. This approach has a reputation as a 'mathematical microscope' in the academic world (Salamalikis *et al.* 2016) because of its ability to reflect the periodic oscillations and multiple change cycles of the research variables hidden in the time series. Wavelet analysis can also better reveal the changing trends of the research system on different time scales and can qualitatively estimate the future development trend of the research object (Cazelles *et al.* 2008). This paper uses the Morlet complex wavelet to study the seasonal variation characteristics of the four seasons and annual precipitation series on the Huang-Huai-Hai Plain. Its mother wavelet is $\psi(t) = e^{ict}e^{-t^2/2}$, the processed data represent the anomaly value, and the wavelet variance is calculated according to the obtained wavelet coefficients. The specific calculation formula is as follows:

$$\mathrm{Var}(a) = \int_{-\infty}^{+\infty} |W_f(a, b)|^2 db \tag{4}$$

where $\mathrm{Var}(a)$ and $W_f(a,b)$ are the wavelet variance and wavelet coefficient, respectively.

Empirical orthogonal function

EOF is a method used to analyse matrix data structure features and extract main data features. It can reflect the spatial distribution characteristics of precipitation fields to a certain extent (Sarkar & Kafatos 2004). Before analysis, the selected data are usually processed into the anomalous form to obtain $X_{m\times n}$, where m is the number of stations and n is the number of years. We decompose the matrix $X_{m\times n}$, that is, $X = \mathrm{EOF}_{m\times m} \times \mathrm{PC}_{m\times n}$ ($\mathrm{EOF}_{m\times n}$ is the eigenvector corresponding to the spatial change, also called the eigenmode; $\mathrm{PC}_{m\times n}$ is the main component corresponding to the time change, also called the time coefficient). To ensure that the modes obtained by the EOF decomposition are independent of each other, the north test method is used (Hannachi *et al.* 2007).

Centre-of-gravity model

The centre-of-gravity model is a concept originally from physics, and it refers to the point through which the resultant force of gravity of the fulcrum of an object in any orientation passes. The concept of the centre of gravity is extended to an area, that is, the regional centre of gravity. The regional centre of gravity, also known as the spatial average, is the extent of the average of a certain geographic element or development element in a two-dimensional space. It refers to the moment when a certain geographic or development element reaches a balance on the spatial plane within a certain period. The regional centre of gravity not only helps in analysing the development process, status, and trend of regional elements but also reflects the spatial fluidity and aggregation of regional elements. The regional centre of gravity is generally calculated by the centre-of-gravity model.

The physics concept of the centre of gravity has been widely used in precipitation, land use, and economic research in recent years, including precipitation barycentres, land use/type centres of gravity, economic aggregate centres of gravity, and population centres of gravity (Gao & Liu 2006; Barmpas *et al.* 2017; Chen *et al.* 2017). The monthly or interannual precipitation barycentre of the area is calculated as follows:

$$\bar{X} = \frac{\sum_{i=1}^{n} X_i P_i}{\sum_{i=1}^{n} P_i}, \quad \bar{Y} = \frac{\sum_{i=1}^{n} Y_i P_i}{\sum_{i=1}^{n} P_i} \tag{5}$$

where $\bar{X}$ and $\bar{Y}$ are the longitude and latitude coordinates, respectively, of the centre of gravity of the monthly or interannual precipitation; X_i and Y_i are the longitude and latitude coordinates, respectively, of the ith weather station; P_i is the monthly or interannual precipitation of the ith weather station; and n is the total number of meteorological stations in the area.

RESULTS AND DISCUSSION

Temporal variation characteristics of precipitation

Precipitation trend analysis

From 1960 to 2019, the precipitation on the Huang-Huai-Hai Plain showed an upward trend in spring and winter and a downward trend in summer and autumn. Only the

winter precipitation trend passed the significance test ($\alpha = 0.1$), showing a significant upward trend. The changing trends of precipitation on the Huang-Huai-Hai Plain from 1960 to 2019 are shown in Table 1.

The trend analysis of the interannual and interdecadal precipitation on the Huang-Huai-Hai Plain was carried out, as shown in Figure 2. The annual precipitation on the Huang-Huai-Hai Plain showed the obvious characteristics of interannual and interdecadal changes, with large interannual fluctuations. From the perspective of interannual changes, the annual precipitation climatic tendency rate of the Huang-Huai-Hai Plain was −5.8 mm/10a from 1960 to 2019. However, the overall downward trend was not significant. From the perspective of interdecadal changes, the average annual precipitation from the 1960s to 1980s showed a decreasing trend. The average annual precipitation from the 1980s to 2000s showed an increasing trend, and then the average annual precipitation began to decrease in the 2010s, but it was still higher than the average annual precipitation in the 1980s. In the past 60 years, the 1980s was the decade with the lowest average annual precipitation, and the 1960s was the decade with the highest average annual precipitation. In the past 10 years, the annual precipitation has shown an overall increasing trend, and the annual precipitation in 2019 declined sharply compared with that in 2018.

Table 1 | Seasonal precipitation trends on the Huang-Huai-Hai Plain during 1960–2019

Time	Normal statistics (Z)	Trend	Significance ($\alpha = 0.1$)
Spring	0.21	Upward	No
Summer	−1.03	Downtrend	No
Autumn	−0.39	Downtrend	No
Winter	1.80	Upward	Yes

Precipitation periodic analysis

The Morlet complex wavelet is used to analyse the periodic seasonal and annual precipitation characteristics of the Huang-Huai-Hai Plain, and the results are shown in Figure 3. The blue colour in the figure indicates that the precipitation is in the rainy cycle, and the yellow colour indicates that the precipitation is in the drier cycle. The wavelet coefficient variance graph can determine the relative intensity of various scale disturbances in a time series, and the corresponding peak is called the main time scale of the series (Mi *et al.* 2005). On the Huang-Huai-Hai Plain, the annual and four seasons were characterized by alternating high–low precipitation. The precipitation anomaly sequence also exhibited periodic characteristics at multiple time scales.

The spring precipitation anomaly sequence on the Huang-Huai-Hai Plain had noticeable periodic changes on the scale of 8–12a and underwent 2.5 alternating cycles of high and low rainfall. There was an obvious peak at 9a in the wavelet variance graph of the spring precipitation anomaly series, indicating that the 9a period, which was the first main period, had the strongest oscillation. The summer precipitation anomaly sequence had noticeable

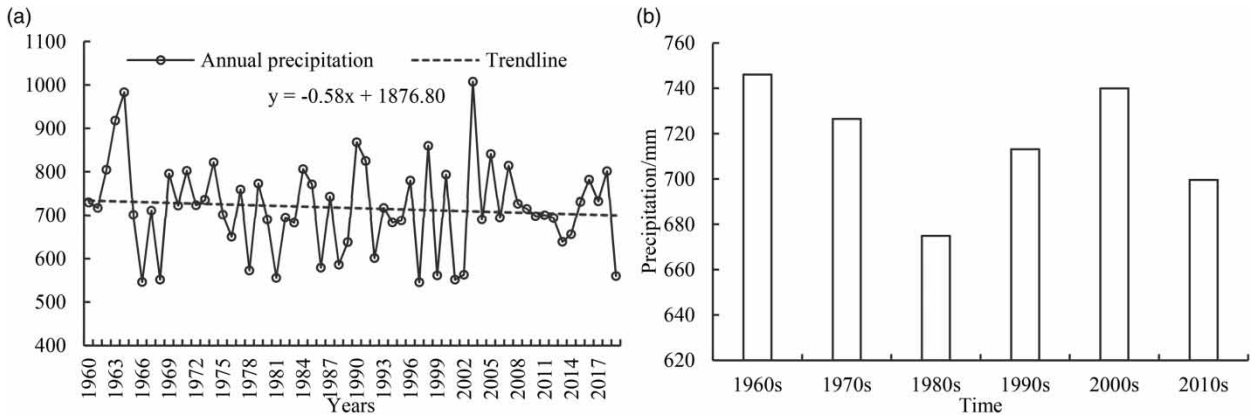

Figure 2 | Interannual (a) and interdecadal (b) precipitation changes on the Huang-Huai-Hai Plain.

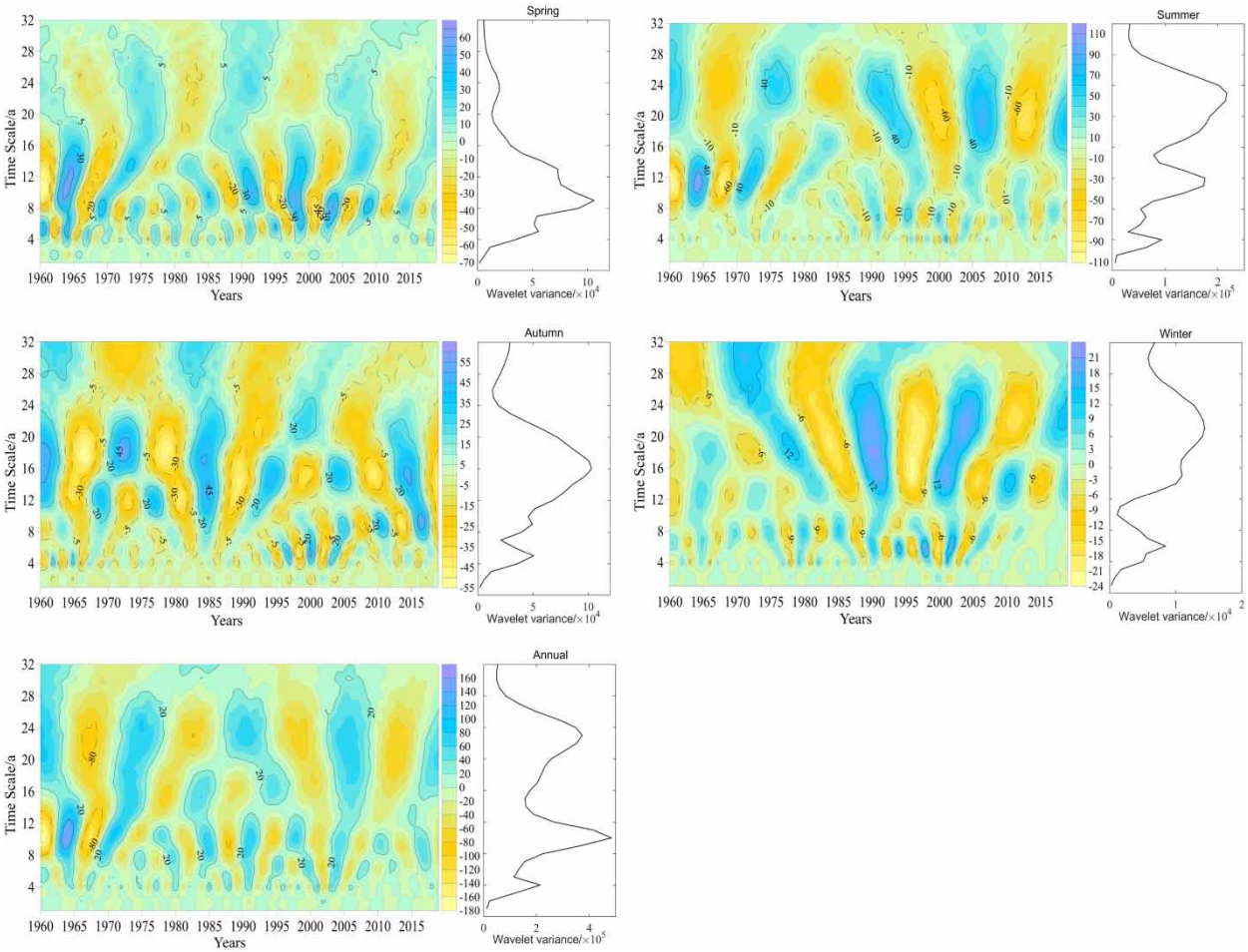

Figure 3 | Wavelet analysis of seasonal and annual precipitation on the Huang-Huai-Hai Plain during 1960–2019. Please refer to the online version of this paper to see this figure in colour: https://doi.org/10.2166/wcc.2021.313.

periodic changes at the scales of 10–14a and 17–23a, both of which experienced 2.5 alternating cycles of high and low rainfall. The first main period was 23a. The autumn precipitation anomaly sequence exhibited noticeable periodic changes at the two scales of 14–18a and 16–21a. It has experienced 3 and 2 alternating cycles of high and low rainfall, respectively. The first main period was 12a. The winter precipitation anomaly sequence had noticeable periodic changes at the two scales of 12–16a and 14–26a, both of which included 1.5 alternating cycles of high and low rainfall. The first main period was 21a. The annual precipitation anomaly sequence on the Huang-Huai-Hai Plain had two-scale change cycles of 8–14a and 21–26a, both of which had 1.5 alternating cycles of high and low rainfall. The first main period was 10a.

Spatial distribution characteristics of precipitation

Spatial distribution of precipitation and its variability

Figure 4(a) shows that the annual precipitation on the Huang-Huai-Hai Plain is unevenly distributed, with more precipitation in the southeast and less precipitation in the northwest. Precipitation generally decreases in a belt-like distribution from the southeast to northwest. The amount of precipitation reflects the different intensities of the East Asian summer monsoon. The areas with high annual average precipitation are mainly located in south-eastern Jiangsu, southern Anhui, and a small part of southern Henan. The precipitation is between 900 and 1,080 mm. The annual average precipitation in Dafeng District, Jiangsu

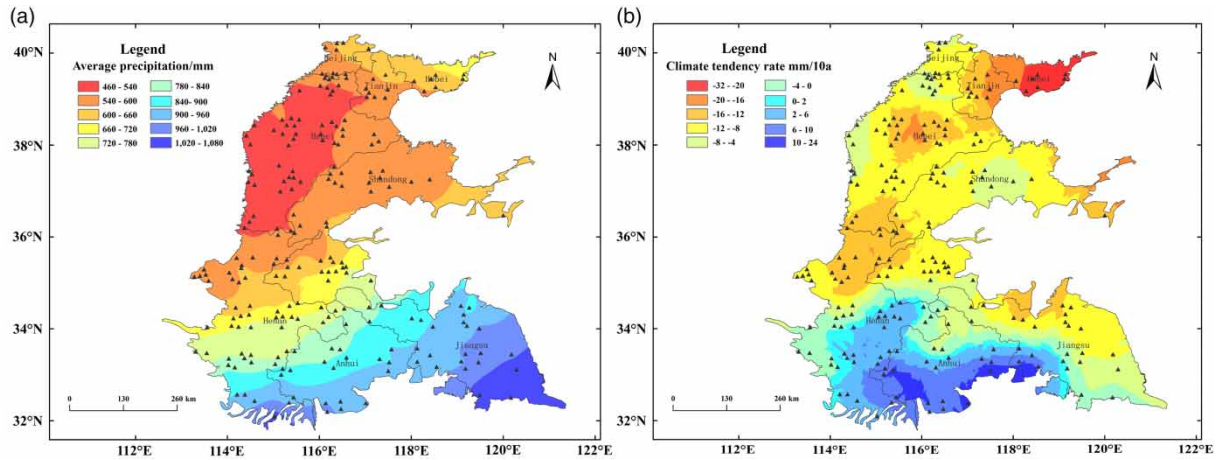

Figure 4 | Spatial distribution of annual precipitation (a) and climate tendency rate (b) on the Huang-Huai-Hai Plain.

Province, is 1,078.1 mm, which is the highest on the Huang-Huai-Hai Plain. The regions with low average yearly precipitation are mainly located in regions of Hebei Province, with precipitation between 460 and 540 mm. The annual average precipitation in Ningjin County, Hebei Province, is 467.0 mm, which is the lowest value on the Huang-Huai-Hai Plain. The difference between the high and low annual average precipitation is 611.1 mm.

Figure 4(b) shows that the annual precipitation on the Huang-Huai-Hai Plain has mainly shown a downward trend in the past 60 years, which is consistent with the above analysis results. The climate tendency rate of precipitation on the Huang-Huai-Hai Plain is mainly distributed in the interval of −32 to 24 mm/10a. The areas of Fuyang and Bengbu in Anhui Province and Huai'an in Jiangsu Province exhibited the largest increase, with values between 10 and 24 mm/10a. The areas of Tangshan and Qinhuangdao in Hebei Province in the north-eastern part of the Huang-Huai-Hai Plain exhibited the largest decrease, between −32 and −20 mm/10a. In general, the climate tendency rate of precipitation on the Huang-Huai-Hai Plain showed the spatial distribution characteristics of increasing in the southwest and decreasing in the northeast.

Spatial distribution pattern of precipitation

To further analyse the spatial distribution characteristics of annual precipitation on the Huang-Huai-Hai Plain, the precipitation anomaly on the Huang-Huai-Hai Plain from 1960 to 2019 was decomposed by EOF. The results are shown in Table 2. According to the North criterion, the error ranges of the first five feature vectors do not overlap and pass the North significance test. The cumulative variance contribution rate is 66.7%, which may represent a significant signal of the precipitation field on the Huang-Huai-Hai Plain in the past 60 years. Because the cumulative variance contribution rate of the first two eigenvectors reached 51.5%, their variance contributions were more considerable than those of the other eigenvectors. Therefore, the critical research and analysis on the distribution of the first two eigenvector fields can better reflect the main spatial distribution characteristics of precipitation on the Huang-Huai-

Table 2 | The variance contribution rate of the first five feature vectors

	First eigenvector	Second eigenvector	Third eigenvector	Fourth eigenvector	Fifth eigenvector
Eigenvalues	2,355,220.1	1,312,774.1	463,874.2	365,304.1	257,486.6
Variance contribution rate (%)	33.1	18.4	6.5	5.1	3.6
Cumulative variance contribution rate (%)	33.1	51.5	58.0	63.1	66.7

Hai Plain. The spatial distribution map of mode 1 and mode 2 of the Huang-Huai-Hai Plain is shown in Figure 5.

The variance contribution rate of the first eigenvector is 33.1%, which is much higher than the contribution rate of the second mode. Thus, it can reflect the main characteristics of spatial precipitation changes on the Huang-Huai-Hai Plain and is a decisive mode. Figure 5(a) shows that the spatial distribution of precipitation is consistent and positive, showing the same phase distribution. The spatial distribution of precipitation changes on the Huang-Huai-Hai Plain shows a 'global pattern', that is, the precipitation distribution characteristics of more or less rainfall throughout the year. The results also show that precipitation of the Huang-Huai-Hai Plain is primarily affected by large-scale weather systems (Baldini *et al.* 2008). The high-value areas of this mode are distributed in Fuyang city, Anhui Province. From the spatial distribution of the precipitation climatic tendency rate (Figure 5(b)), it can be seen that the annual precipitation climatic tendency rate in Fuyang city is relatively high, and both droughts and floods are very sensitive. The low-value regions are mainly distributed in Baoding city and Langfang city, Hebei Province.

The variance contribution rate of the second eigenvector is 18.4%. Figure 5(b) shows that the precipitation characteristics of the Huang-Huai-Hai Plain show a north-south reverse distribution pattern. The spatial distribution of precipitation changes on the Huang-Huai-Hai Plain has a 'north-south pattern', that is, less (more) in the north and more (less) in the south. The zero contour is at approximately 35°N. The positive high-value areas of this mode are mainly distributed in the northern and eastern regions of Hebei Province. Negative high-value areas are distributed in southern Jiangsu Province and southwestern Anhui Province. The Huang-Huai-Hai Plain is located in a region with obvious monsoon climate. Due to the blocking and uplifting of mountains and the prevailing northerly wind in winter, precipitation is easy to form in the north. Affected by the East Asian monsoon in summer, it is easy to cause precipitation in the southern region. The spatial distribution of precipitation changes on the north and south of the Huang-Huai-Hai Plain reflects its monsoon climate characteristics to a certain extent (Zhu *et al.* 2000).

Distribution characteristics of precipitation barycentres

Taking the precipitation at the 215 stations from 1960 to 2019 as the weights, the latitude and longitude coordinates of the precipitation barycentres are calculated on the Huang-Huai-Hai Plain. The locations and movement tracks of the precipitation barycentres on the Huang-Huai-Hai Plain are shown in Figure 6. The precipitation barycentres are not randomly distributed but are found mainly in Jining city and Taian city, Shandong Province. They are located between 35°0–36°9′N and 116°6–116°32′E on the east-central Huang-Huai-Hai Plain. The standard deviation ellipse tool in ArcGIS was used to create a first-level

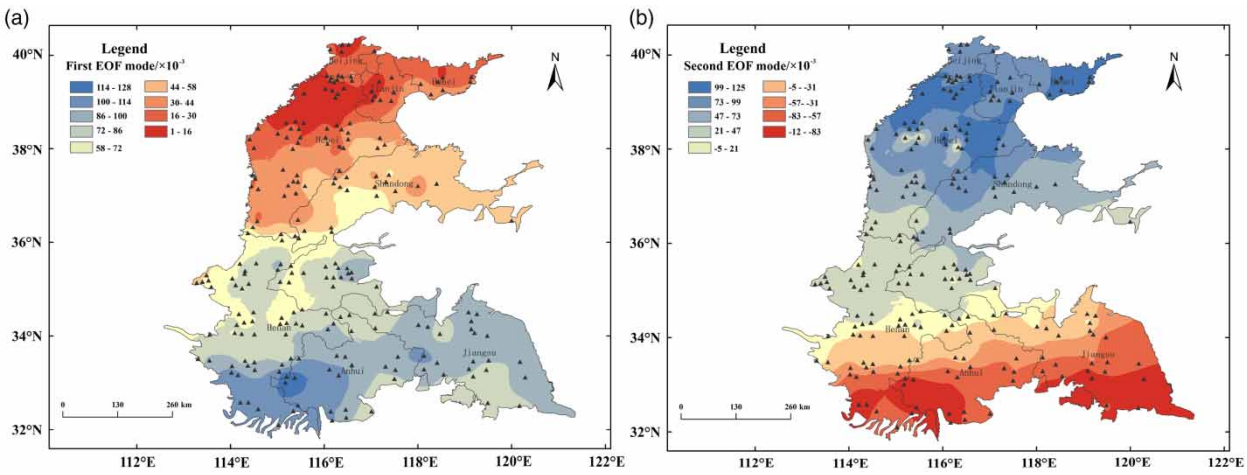

Figure 5 | Distributions of two eigenvectors of precipitation on the Huang-Huai-Hai Plain before EOF expansion.

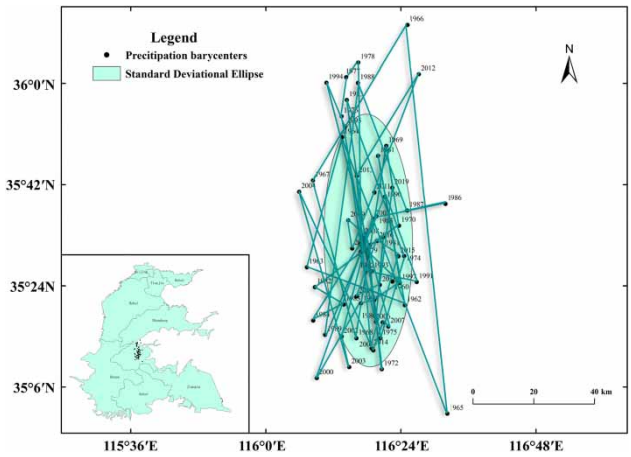

Figure 6 | The locations and movement tracks of precipitation barycentres on the Huang-Huai-Hai Plain during 1960–2019.

standard deviation ellipse with 60 precipitation gravity points. The direction of the standard deviation ellipse was 1.04° west of the north. The major axis of the ellipse was located in the north–south direction, and the length was 81.52 km, indicating that the spatial distribution pattern of the precipitation barycentres was oriented in the south–north direction. The minor axis of the ellipse was oriented in the east–west direction, the length was 24.14 km, and the oblateness of the ellipse was 0.70, indicating that the distribution of the precipitation barycentres on the Huang-Huai-Hai Plain had obvious directionality and that the degree of dispersion was small. These results also showed that the fluctuations in annual precipitation were more significant in the north–south direction. The annual average precipitation on the Huang-Huai-Hai Plain was higher in the southeast and lower in the northwest. The precipitation in the southern region was between 960 and 1,080 mm, which had a greater weight, and the latitude difference between the north and south was large. Therefore, the degree of influence of the East Asian monsoon changed greatly, which may have led to the spatial distribution pattern of the precipitation barycentres in the north–south direction.

To further analyse the changes in the longitude and latitude of the precipitation barycentres on the Huang-Huai-Hai Plain, a map of the changes in the longitude and latitude coordinates of the precipitation barycentres from 1960 to 2019 was drawn (Figure 7). We used the M-K method to test the significance of changes in the latitude and longitude of the precipitation barycentres. Figure 7(a) illustrates that the longitudes of the annual precipitation barycentres on the Huang-Huai-Hai Plain showed a downward trend during 1960–2019. The M-K trend test value was −0.096, which failed the 90% reliability test and indicated a non-significant downward trend. The longitudes of the precipitation barycentres in the past 60 years had a maximum value of 116.54° and a minimum value of 116.10°. The longitudes of the precipitation barycentres in the 1960s and 1980s fluctuated greatly, while the fluctuation range in the past 10 years was relatively small. Figure 7(b) illustrates that the latitudes of the precipitation barycentres on the Huang-Huai-Hai Plain showed an overall downward trend, and the M-K trend test value was −0.695, which failed the 90% reliability test. Therefore, the latitudes of the precipitation barycentre generally had a nonsignificant downward trend. In the past 60 years, the maximum latitude of the precipitation barycentres was 36.17°, and the minimum was 35.02°; thus, the difference was 1.15°, and there were large fluctuations. In summary, the precipitation barycentres on

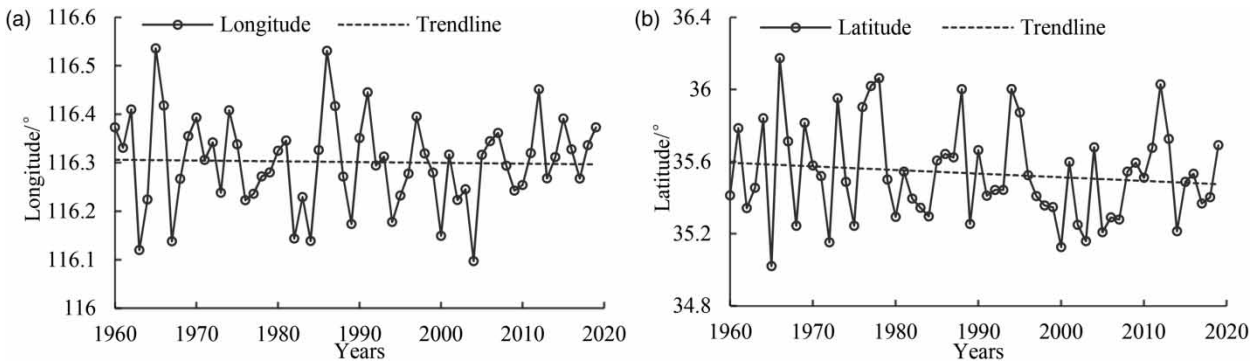

Figure 7 | Changes in the latitude (b) and longitude (a) coordinates of the precipitation barycentres during 1960–2019.

the Huang-Huai-Hai Plain tended to move southwest from 1960 to 2019, but the overall trend was not obvious. The above-mentioned migration phenomenon of the annual precipitation barycentre on the Huang-Huai-Hai Plain has a lot to do with the amount of precipitation and the latitude and longitude of each meteorological station (Chen *et al.* 2017). At the same time, the Huang-Huai-Hai Plain is located on the edge of the monsoon climate zone, and the precipitation is not only affected by the East Asian monsoon but also by the mid-high latitude circulation to a large extent (Li *et al.* 2020). As shown in Figure 5(b) in the previous section, the precipitation variability on the Huang-Huai-Hai Plain in the past 60 years shows an increase in the southwest and a decrease in the northeast, which may cause the precipitation barycentre to move to the southwest. The precipitation barycentre on the Huang-Huai-Hai Plain moves to the southwest. On the one hand, it is beneficial to guarantee the grain output of Henan, Anhui, and other major grain production areas on the southwest of the Huang-Huai-Hai Plain. On the other hand, it has exacerbated the drought and water shortage in Beijing, Hebei, and Tianjin on the Northeast of the Huang-Huai-Hai Plain, and has increased the water supply pressure on the east route of the South-to-North Water Diversion (Sun 2019).

Temporal and spatial distributions of precipitation on the Huang-Huai-Hai Plain are mainly affected by geographic location, topographic conditions, and atmospheric circulation (Fu 1992; Zhang *et al.* 2003; Zhong 2020). The geographic location and topographic conditions can be considered constant factors, but the atmospheric circulation varies significantly from year to year with interdecadal changes. Therefore, the geographic location determines the average magnitude of precipitation on the Huang-Huai-Hai Plain. The interaction between topographic conditions and atmospheric circulation causes the spatial distribution of precipitation on this plain to present certain characteristics (You *et al.* 2013). Atmospheric circulation, especially anomalous changes in the East Asian summer monsoon and subtropical high pressure, will cause obvious anomalies in precipitation on the Huang-Huai-Hai Plain (Cai *et al.* 2003; Hao 2011). The subtropical high is northerly, and the summer monsoon is more vigorous. The Huang-Huai-Hai Plain has more precipitation and vice versa. The ENSO is one of the strongest signals of sea–atmosphere coupling observed to date (Rasmusson & Michael 1985), and it is a crucial factor causing irregular atmospheric circulation in the mid-high latitudes of East Asia and anomalous East Asian summer monsoon precipitation (Zhang *et al.* 2013; Kim *et al.* 2017). The Huang-Huai-Hai Plain is within the Asian monsoon region, and its response to ENSO precipitation is very robust (Lu & Zhang 1995). In general, during the development stage of ENSO events, the Yangtze Plain in China has more precipitation, while the Huang-Huai-Hai Plain has less precipitation and more drought (Liu *et al.* 2005a, 2005b; Zhang *et al.* 2006). According to the latest research by the National Climate Centre (http://cmdp.ncc-cma.net/pred/cn_enso.php), an El Niño event has officially formed in 2020 (weak intensity). Affected by this El Niño event, in the summer of 2020, the intensity of the subtropical high in the western Pacific will be relatively strong, and the precipitation in China will generally be distributed in a spatial pattern of 'more in the north and south and less in the middle'. Higher precipitation occurs in summer, and floods are stronger than droughts. It is expected that the precipitation barycentre in 2020 will continue to shift to the north.

CONCLUSIONS

(1) The annual precipitation on the Huang-Huai-Hai Plain exhibited obvious interannual and interdecadal changes. The precipitation showed an upward trend in spring and winter and a downward trend in summer and autumn. The precipitation in winter exhibited a significant upward trend. Annual and seasonal precipitation on the Huang-Huai-Hai Plain had obvious periodic characteristics of multiyear changes. In the research time period, most of them experienced 1.5 or 2.5 alternating cycles of high and low rainfall. In terms of primary cycles, the first main periods of the precipitation sequence in spring, summer, autumn, and winter were 9a, 23a, 12a, and 21a, respectively. The first main period of the annual precipitation series was 10a.

(2) The annual precipitation on the Huang-Huai-Hai Plain was unevenly distributed. The precipitation showed a zonally decreasing distribution from the southeast to northwest. The climate tendency rate of the Huang-Huai-Hai Plain was distributed in the interval of −32

to 24 mm/10a. The largest increase in precipitation occurred in Fuyang city and Bengbu city in Anhui Province. The largest decrease in precipitation occurred in Tangshan city and Qinhuangdao city in Hebei Province. The application of the EOF method revealed the temporal and spatial distribution characteristics of the precipitation field. There were two main types of spatial distributions of annual precipitation on the Huang-Huai-Hai Plain: a 'global pattern' and a 'north-south pattern'. The 'global pattern' is a decisive mode.

(3) The interannual precipitation barycentres on the Huang-Huai-Hai Plain were distributed in Jining city and Taian city, Shandong Province. The spatial distribution pattern of the precipitation barycentres was in the south–north direction as a whole, with a small degree of dispersion and obvious directionality. In the past 60 years, the longitudes and latitudes of the interannual precipitation barycentres showed a nonsignificant decrease. Therefore, the precipitation barycentres generally moved to the southwest, but the trend was not obvious. It is expected that the precipitation barycentre in 2020 will continue to shift to the north.

ACKNOWLEDGEMENTS

This study was supported by the National Natural Science Foundation of China (No. 52079125) and Henan Natural Science Foundation (No. 182300410139).

DATA AVAILABILITY STATEMENT

All relevant data are included in the paper or its Supplementary Information.

REFERENCES

An, H., Yan, J., Zhang, T. & Lao, G. 2013 Temporal and spatial characteristics of extreme precipitation events in North China Plain on background of climate warming. *Bulletin of Soil and Water Conservation* **33** (3), 144–148.

Aziz, O. & Burn, D. H. 2005 Trends and variability in the hydrological regime of the Mackenzie River Basin. *Journal of Hydrology* **319**, 282–294.

Baldini, L., McDermott, F., Foley, A. & Baldini, J. 2008 Spatial variability in the European winter precipitation delta δ^{18}O-NAO relationship: implications for reconstructing NAO-mode climate variability in the Holocene. *Geophysical Research Letters* **35**, 4.

Barmpas, G., Kopsacheilis, A. & Politis, I. 2017 Small scale intervention in a major city center interchange: economic, environmental and sustainability analysis. *Transportation Research Procedia* **24**, 41–49.

Cai, X., Gao, J. & Wu, B. 2003 Diagnostic analysis of the influence of summer East Asian monsoon and western Pacific subtropical high on drought and flood in Fujian. *Journal of Applied Meteorological Science* **14** (03), 322–330.

Cazelles, B., Chavez, M., Berteaux, D., Menard, F., Vik, J., Jenouvrier, S. & Stenseth, N. 2008 Wavelet analysis of ecological time series. *Oecologia* **156**, 287–304.

Chen, S., Li, L. & Li, J. 2017 Analysis of the temporal and spatial variation characteristics of precipitation in the Lancang River Basin over the past 55 years. *Journal of Geo-Information Science* **19** (03), 365–373.

Costa, A. C. & Soares, A. 2009 Trends in extreme precipitation indices derived from a daily rainfall database for the South of Portugal. *International Journal of Climatology* **29**, 1956–1975.

Fang, J., Guo, B., Zhang, Z., Chen, Z. & Wang, X. 2018 Temporal and spatial characteristics of precipitation extremes on the Huang-Huai-Hai Plain during 1960–2013. *Journal of Henan University (Natural Science)* **48** (02), 160–171.

Fu, B. 1992 The influence of terrain and altitude on precipitation. *Acta Geographica Sinica* (04), 302–314.

Gao, Z. & Liu, J. 2006 The LUCC responses to climatic changes in China from 1980 to 2000. *Acta Geographica Sinica* **61** (08), 865–872.

Hannachi, A., Jolliffe, I. & Stephenson, D. 2007 Empirical orthogonal functions and related techniques in atmospheric science: a review. *International Journal of Climatology* **27** (9), 1119–1152.

Hao, L. 2011 *Spatial-Temporal Variation of the Precipitation in North China and the Impact Factors of Precipitation Reduction*. Nanjing University of Information Technology, Nanjing.

Kim, J., Son, C., Moon, Y. & Lee, J. 2017 Seasonal rainfall variability in Korea within the context of different evolution patterns of the central Pacific El Niño. *Journal of Water and Climate Change* **8** (03), 412–422.

Li, T. & Luo, J. 2011 Projection of future precipitation change over China with a high-resolution global atmospheric model. *Advances in Atmospheric Sciences* **28** (2), 464–476.

Li, C., Xiao, Z. & Zhang, X. 2012 Climatic characteristics of regions of China for precipitation in various the past 60 years. *Meteorological Monthly* **38** (4), 419–424.

Li, X., Ju, H., Garre, S., Yan, C., William, D. & Liu, Q. 2017 Spatiotemporal variation of drought characteristics on the Huang-Huai-Hai Plain, China under the climate change scenario. *Journal of Integrative Agriculture* **16**, 2308–2322.

Li, Y., Xie, Z., Qin, Y. & Zhou, S. 2018 Spatio-temporal variations in precipitation on the Huang-Huai-Hai Plain from 1963 to 2012. *Journal of Earth System Science* **127**, 7.

Li, T., Zhou, Z., Fu, Q., Liu, D., Li, M., Hou, R., Pei, W. & Li, L. 2020 Analysis of precipitation changes and its possible reasons in Songhua River Basin of China. *Journal of Water and Climate Change* **11** (03), 839–864.

Liu, B., Xu, M., Henderson, M. & Qi, Y. 2005a Observed trends of precipitation amount, frequency, and intensity in China, 1960–2000. *Geophysical Research* **110**, D08103.

Liu, C., Zhang, Q., Xu, Y. & Jiang, P. 2005b Impacts of ENSO events on climatic changes during last 50 years in the Yangtze Delta. *Meteorological Monthly* **31** (03), 12–16.

Lu, D. & Zhang, X. 1995 Characteristics of China's precipitation and temperature response to ENSO. *Journal of Applied Meteorological Science* **6** (1), 118–123.

Luo, H., Li, C., Wei, J., Hou, C. & Ma, G. 2015 Accuracy validation of TRMM precipitation data in Shaxi River Basin. *Journal of Subtropical Resources and Environment* **10** (04), 69–76.

Mi, X., Ren, H., Yang, Z., Wei, W. & Ma, K. 2005 The use of the Mexican Hat and the Morlet wavelets for detection of ecological patterns. *Plant Ecology* **179**, 1–19.

Pirnia, A., Golshan, M., Darabi, H., Adamowski, J. & Rozbeh, S. 2019 Using the Mann-Kendall test and double mass curve method to explore stream flow changes in response to climate and human activities. *Journal of Water and Climate Change* **10** (4), 725–742.

Qian, W., Fu, J. & Yan, Z. 2007 Decrease of light rain events in summer associated with a warming environment in China during 1961–2005. *Geophysical Research Letters* **34**, L11705.

Rasmusson, E. & Michael, H. 1985 El Niño and variations in climate. *American Scientist* **73** (02), 168–177.

Ren, G., Guo, J., Xu, M., Chu, Z., Zhang, L., Zhou, X., Li, Q. & Liu, X. 2005 Climate changes of China's mainland over the past half century. *Acta Meteorologica Sinica* **63** (6), 942–956.

Rong, Y. & Luo, J. 2009 Evolution of climate change intensity in North China from 1901 to 2002. *Journal of Hohai University (Natural Sciences)* **37** (3), 276–280.

Salamalikis, V., Argiriou, A. & Dotsika, E. 2016 Periodicity analysis of delta O-18 in precipitation over Central Europe: time-frequency considerations of the isotopic 'temperature' effect. *Journal of Hydrology* **534**, 150–163.

Sarkar, S. & Kafatos, M. 2004 Interannual variability of vegetation over the Indian sub-continent and its relation to the different meteorological parameters. *Remote Sensing of Environment* **90** (2), 268–280.

Sun, Z. 2019 Analysis on the characteristics of precipitation and runoff in the source area of the east route of the South-to-North Water Transfer Project. *Journal of Water Resources and Water Engineering* **30** (04), 86–91.

Worku, T., Khare, D. & Tripathi, S. 2019 Spatiotemporal trend analysis of rainfall and temperature, and its implications for crop production. *Journal of Water and Climate Change* **10** (4), 799–817.

Wu, J., Liu, X., A, L. V., Zhao, L. & Liu, M. 2011 Analysis of the temporal and spatial layout of drought in the Huang-Huai-Hai Region. *China population Resources and Environment* **21** (2), 100–105.

Yang, J., Mei, X., Huo, Z., Yan, C., Ju, H., Zhao, F. & Liu, Q. 2015 Water consumption in summer maize and winter wheat cropping system based on SEBAL model in Huang-Huai-Hai Plain China. *Journal of Integrative Agriculture* **14**, 2065–2076.

You, Q., Kang, S., Ren, G., Fraedrich, K., Pepin, N., Yan, Y. & Ma, L. 2011 Observed changes in snow depth and number of snow days in the eastern and central Tibetan Plateau. *Climate Research* **46**, 171–183.

You, L., Cheng, Y., Li, H. & Ta, L. 2013 Abnormal precipitation and its circulation characteristics during June to August from 1961 to 2012 in Inner Mongolia Autonomous Region. *Journal of Meteorology and Environment* **29** (06), 56–62.

Yu, P., Yang, T. & Wu, C. 2002 Impact of climate change on water resources in southern Taiwan. *Journal of Hydrology* **260**, 161–175.

Yuan, Y., Yan, D., Yuan, Z., Yin, J. & Zhao, Z. 2019 Spatial distribution of precipitation in Huang-Huai-Hai River Basin between 1961 to 2016, China. *International Journal of Environmental Research and Public Health* **16** (18), 3404.

Zhang, Q., Tao, S. & Chen, L. 2003 The interannual variation of East Asian summer monsoon index and East Asian atmospheric circulation. *Acta Meteorologica Sinica* **61** (05), 559–568.

Zhang, R., Yin, Y., Li, Q., Liu, Y. & Niu, T. 2006 Utilizing ARGO data to improve the prediction of ENSO and short-term climate prediction of summer rainfall in China. *Journal of Applied Meteorological Science* **17** (05), 538–547.

Zhang, A., Gao, X. & Ren, G. 2008 Characteristic of extreme precipitation events change in central North China in recent 45 years. *Arid Meteorology* **26** (4), 46–50.

Zhang, X., Chen, S., Sun, H., Shao, L. & Wang, Y. 2011 Changes in evapotranspiration over irrigated winter wheat and maize in North China Plain over three decades. *Agricultural Water Management* **98**, 1097–1104.

Zhang, Q., Li, J., Singh, V., Xu, C. & Deng, J. 2013 Influence of ENSO on precipitation in the East River basin, south China. *Journal of Geophysical Research: Atmospheres* **118** (5), 2207–2219.

Zhang, D., Yan, D., Wang, Y., Lu, F. & Wu, D. 2015 Changes in extreme precipitation in the Huang-Huai-Hai River basin of China during 1960–2010. *Theoretical and Applied Climatology* **120**, 195–209.

Zhong, S. 2020 Advances in the study of the influencing mechanism and forecast methods for orographic precipitation. *Plateau Meteorology* **39** (05), 1122–1132.

Zhu, C., He, J. & Wu, G. 2000 East Asian monsoon index and its interannual relationship with large scale thermal dynamic circulation. *Acta Meteorologica Sinica* **58** (04), 391–402.

First received 13 November 2020; accepted in revised form 4 February 2021. Available online 2 March 2021